Desalination and Water Treatment
www.deswater.com

1944-3994/1944-3986 © 2012 Desalination Publications. All rights reserved
doi: 10.1080/19443994.2012.719475

50 (2012) 264–271
December

Taylor & Francis
Taylor & Francis Group

Parametric study on phenol photocatalytic degradation under pure visible and solar irradiations by Fe-doped TiO_2

Tarek S. Jamil[a,]*, Tarek A. Gad-Allah[a], Montaser Y. Ghaly[b]

[a]*Water Pollution Control Department, National Research Center, 33 El-Behouth St., P.O. Box 12311, Dokki, Cairo, Egypt*
Tel. +201223763699; Fax: +20233371479; email: omaytarek73@yahoo.com
[b]*Chemical Engineering and Pilot Plant Department, National Research Center, 33 El-Behouth St., P.O. Box 12311, Dokki, Cairo, Egypt*

Received 8 March 2012; Accepted 18 July 2012

ABSTRACT

Fe-doped TiO_2 photocatalysts of different Fe/Ti molar ratios were successfully prepared using wet impregnation method. Prepared Fe-doped TiO_2 photocatalysts were characterized by X-ray diffraction, scanning electronic microscope and specific surface area analysis. All the Fe-doped TiO_2 photocatalysts possess only anatase crystal structure with no peaks relevant to iron. The activity of the Fe-doped TiO_2 photocatalyst for the degradation of phenol was investigated under solar and visible lights and under different reaction conditions, e.g. doping ratio, catalyst concentration and hydrogen peroxide concentration. The degradation rate under solar irradiation was much higher than that under visible light irradiation. 0.05% Fe/Ti molar ratio was the optimum doping ratio for phenol degradation under solar as well as visible light. Photocatalyst of this doping ratio showed higher activity than P25 TiO_2 under solar light irradiation and visible irradiation which might be due to electron-hole separation by iron.

Keywords: Photocatalysis; Phenol; Solar light; Pure visible light; Degradation

1. Introduction

Titanium dioxide has been proved to be the most suitable photocatalyst for widespread environmental applications because of its biological and chemical inertness, strong oxidizing power, non-toxicity and long-term stability against photo and chemical corrosion [1,2]. However, TiO_2 can be activated only under UV light of wavelengths <387 nm irradiation due to its large band gap of 3.2 eV. The solar spectrum contains about 4% UV light only. Owing to this inherent limitation, the solar energy cannot be utilized efficiently in the photocatalytic process [3,4]. The photocatalytic activity of TiO_2 usually depends on a competition between two processes, (1) the ratio of the transfer rate of surface charge carriers from the interior to the surface and (2) the recombination rate of photo-generated electrons and holes. If the recombination of photo-generated electrons and holes occurs too fast (<0.1 ns), then there is not enough time for any other chemical reaction to occur. Compared with other semiconductor, the surface charge carriers of TiO_2 are relatively long-lived (around 250 ns), allowing the electrons or holes to travel to the crystallite surface. It is on the TiO_2 surface that different types of radicals are formed. The most common radicals are the $^{\cdot}OH$ radicals, which are then free to carry out other chemical reactions on the surface of TiO_2 [5]. In order to extend its light absorption into visible-light

---

*Corresponding author.

region, and also to reduce the recombination of photo-generated electrons and holes, various metal and non-metal ions have been doped into TiO_2 [6]. Among various transition metal ions, Fe^{3+} was proved as successful doping element due to its half-filled electronic configuration. It has been reported that a proper concentration of Fe^{3+} ions in TiO_2 is not only to favour electron–hole separation, but also to narrow its band gap [7]. The photocatalytic activity of TiO_2 must be further enhanced from practical point of view of use and commerce. In order to achieve this, Fe-doped TiO_2 has attracted much attention [8].

The objective of this investigation was to synthesize iron-doped TiO_2 by wet impregnation method with elevated activity. The photocatalytic activity of prepared photocatalyst was assessed against phenol degradation as phenol is an important by-product in different industrial sectors such as pulp and paper mill, petroleum refineries, petrochemical, textile, leather, rubber industry, fiberglass manufacturing and paint manufacturing [9]. Also, kinetic studies of phenol degradation were carried out through this study.

2. Experimental

2.1. Preparation and characterization of iron doped TiO_2

Iron-doped TiO_2 of different iron molar ratios (ranging from 0 to 0.1% Fe/Ti) were prepared from TiO_2 powder (Degussa Co. Ltd, Germany) and analytical grade $FeCl_3$ (Aldrich, Germany), as precursor of iron, using wet impregnation method. At first, TiO_2 powder was impregnated in aqueous solutions of $FeCl_3$ containing the required amount of iron. The suspension was then stirred for about 3 h at 60°C and finally dried at 100°C. The resulted powder was finely ground in a mortar and calcined at 300°C for about 2 h. As a blank sample, TiO_2 was also treated in the same way but in the absence of iron.

The X-ray diffraction (XRD) patterns of prepared samples were collected at room temperature by a Philips powder diffractometer using Cu K_α radiation and a 2θ scan rate of 2°/min. Whereas, specific surface areas were calculated using Brunauer-Emmet-Edward (BET) equation applied on isotherms collected from Flow Sorb 2300 apparatus (Micromeritics).

2.2. Photocatalytic efficiency tests

The photocatalytic activity of prepared samples was evaluated by the degradation of phenol in an aqueous solution. Pure visible light was supplied by two general electric (GE) energy-saving 125-W indoor halogen lamps "Philips" floodlight purchased locally. The incidence of the visible light was perpendicular to the surface of the solution. The distance between the surface of the solution and the light source was 10 cm. The intensity of the lamp (400–580 nm wavelengths) was nearly constant during the experiments.

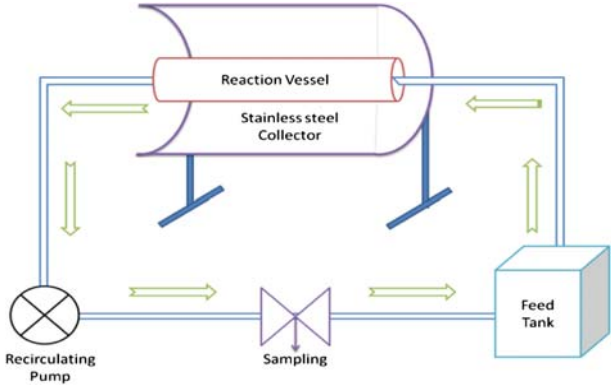

Fig. 1. Schematic diagram of the solar photocatalytic oxidation unit.

2.3. Solar light experiments

All solar photocatalytic experiments were carried out under similar conditions on sunny days of summer (July) under clear skies between 11 am and 3 pm. The photocatalytic oxidation was carried out in aqueous suspensions of the prepared Fe-doped-TiO_2 irradiated by sunlight which was focused on the photoreaction system. The mixture was continuously fed to the solar reactor from the feed tank by means of a peristaltic pumps batch process. The solution flow rate, maintained constant for all of the runs, was 60 L/h. The total irradiated volume was 3.5 L. The schematic diagram of the experimental set-up is shown in Fig. 1.

3. Results and discussion

3.1. Characterization of prepared samples

XRD was used to investigate the phase structure of prepared iron doped TiO_2 powders heat treated at 300°C/2 h. The recorded XRD patterns are presented in Fig. 2. It can be seen that the diffraction peaks of all samples belong to anatase phase. It is interesting to note that iron oxides or Fe_xTiO_y phases were not detected in the patterns of XRD. One probable reason is that the concentration of Fe-doping is so low that it cannot be detected by XRD. The other reason might be that the radii of Ti^{4+} (0.68 Å) and Fe^{3+} (0.64 Å) ions are very similar and all the iron ions may be inserted

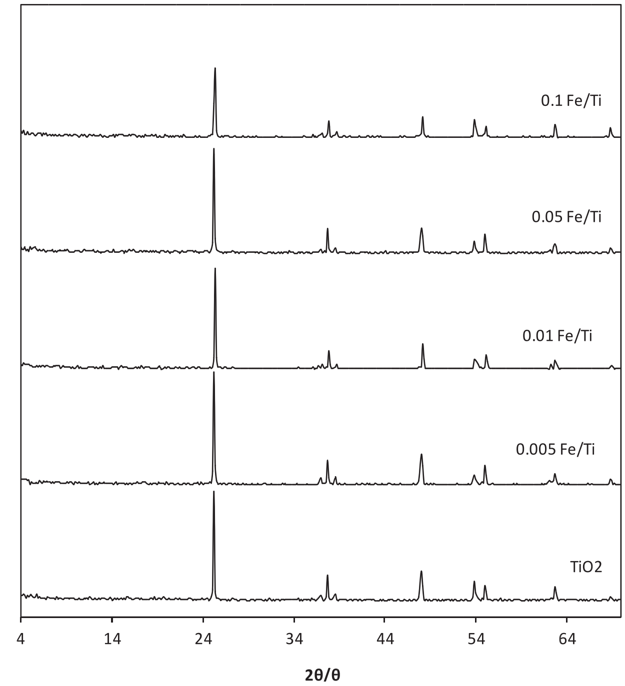

Fig. 2. XRD patterns of prepared photocatalysts of different Fe/Ti atomic ratios.

into the structure of titania, and located at interstices or occupy some of the titania lattice sites, forming an iron–titanium oxide solid solution. As shown for the (1 0 1) peak, a slight shift in the peak position (from 25.32° for Fe/Ti = 0 to 25.39° of Fe/Ti = 0.1) was observed after the introduction of Fe^{3+}, indicating the occurrence of very slight lattice distortion in the anatase structure. This observation is similar to other previous studies [10–12]. The lattice distortion was caused by second probability stated above, i.e. the substitution of part of the Ti site by Fe ions, which suggests the formation of the solid solution of Fe-doped TiO_2. Since the radii of Fe^{3+} and Ti^{4+} are very similar [13], it is easy for Fe^{3+} ions to cooperate with the matrix of the TiO_2 particles without causing a significant crystalline distortion.

Furthermore, with the increase in Fe concentration, peak intensities of anatase slightly decrease and the peak width of (1 0 1) plane of anatase ($2\theta = 25.3°$) becomes broader. Therefore, it is reasonable to deduce that the larger the amount of Fe-doping, the poorer the crystallization of the TiO_2 powders, and the smaller the crystallite size of TiO_2. The average crystallite size, *L*, was estimated from the full width at half maximum (FWHM) of the (1 0 1) peak according to Debye-Scherrer's equation [14]:

$$L = K\lambda/\beta \cos\theta$$

where *L* is the crystallite size, λ is the wavelength of the XRD (Cu $K_\alpha = 1.5406$ Å), K is the shape factor (usually taken as 0.89) and β is the line width at half-maximum height. The calculated crystal sizes at (1 0 1) plane were 130, 102.4, 112.2, 108.3 and 107.7 nm for Fe/Ti weight ratios 0, 0.005, 0.01, 0.05 and 0.1%, respectively (Fig. 3). This result shows that the increasing amount of doped Fe retards the crystal growth of the anatase TiO_2 during heat treatment which is consistent with Wang et al. [15] work; the larger the amount of Fe^{3+}-doping, the wider the width of the diffraction peaks, the worse the crystallization, and the smaller the grain size of TiO_2 powders.

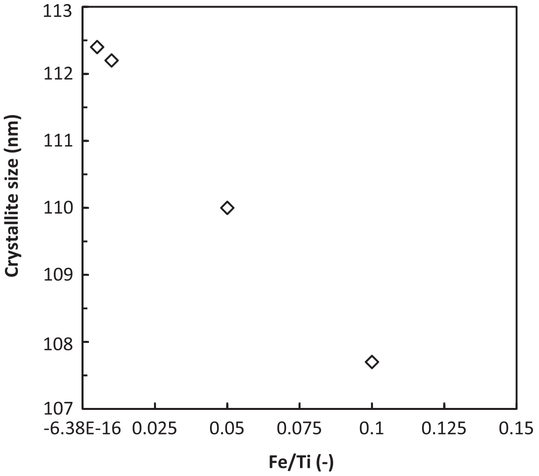

Fig. 3. Effect of Fe/Ti doping ratio on the crystallite size of TiO_2.

The specific surface areas of the samples were measured using BET method by N_2 adsorption and desorption at 77 K. There was not much difference in surface areas since the prepared samples showed a specific surface areas of 33.07, 38.21, 33.94, 33.51 and 34.73 m^2/g of Fe-doped concentration (0, 0.005, 0.01, 0.05 and 0.1% weight Fe) respectively.

3.2. *Effect of Fe/Ti weight ratio on photocatalytic oxidation of phenol under solar and visible light*

It is necessary to separately irradiate visible and UV lights to illustrate the response of prepared photocatalysts to these sources of lights and to compare the response with that of commercially available TiO_2. In Fig. 4 the heterogeneous mixtures of phenol with Fe^{3+}-doped and undoped TiO_2 were separately exposed to pure visible radiation and sunlight during sunny days. Based on the linear relationship, the degradation of phenol followed the pseudo-order kinetics as depicted by ($\mathrm{Ln}\, C_t/C_0 = k_{\mathrm{obs}}\, t$), where k_{obs} is

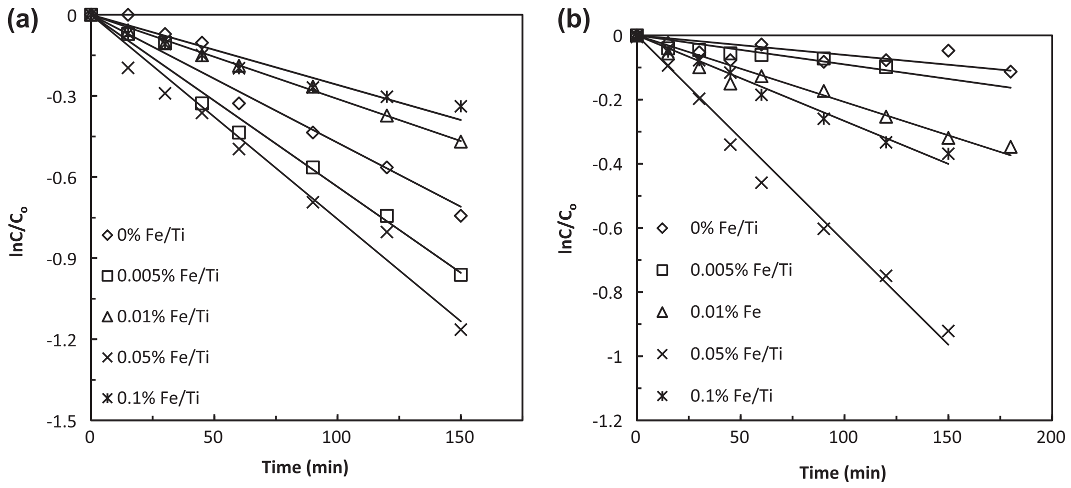

Fig. 4. Pseudo-first-order kinetics of phenol degradation using different Fe/Ti weight ratios under (a) solar radiation and (b) pure visible light.

the observed rate constant, and C_0 and C_t are the concentrations of phenol at $t = 0$ and t, respectively. The calculated k_{app} are plotted against Fe/Ti doping ratio in Fig. 5 in order to more clearly understand the effect of doping ratio (Fe/Ti = 0–0.1%). The results obviously showed that under both pure visible and sunlight irradiations, the rate constant of phenol degradation increased to attain a maximum value at 0.05% Fe/Ti and then decreased with the increase in the Fe content, i.e. 0.05% doping ratio is the optimum. At this optimum doping amount of Fe, the rates under pure visible and solar light were greater than that of undoped TiO_2. Therefore, it is very characteristic that the Fe^{3+}-doped TiO_2 showed a visible light response. It is known that the photocatalytic activity of doped TiO_2 depends on its light absorption ability, the amount of dopant, charge trapping by the dopant and the recombination of electron–holes and crystallite size.

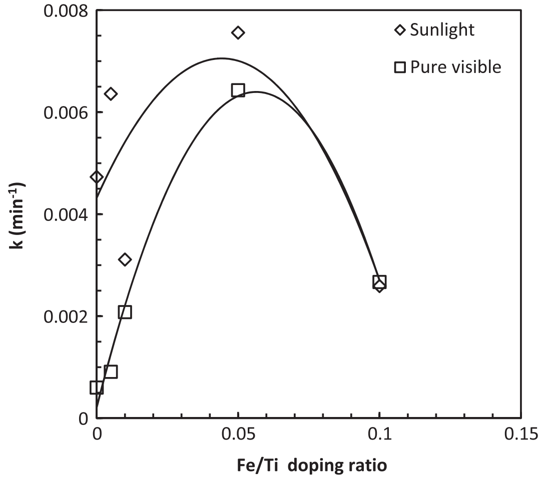

Fig. 5. Change in pseudo-first order rate constant of phenol degradation using different Fe/Ti doping ratios under sunlight and pure visible light.

In order to explain the enhanced visible-light-activity of the Fe-doped TiO_2, several possible mechanisms were proposed. As shown in Fig. 6, with the substitution of Ti^{4+} by Fe^{3+} in the crystal structure of TiO_2 (which was proved by peak shifting in XRD pattern), new Fe levels are introduced between the conduction and valence band of TiO_2, then the electrons can be promoted to the conduction band from Fe levels. The electrons can also be promoted from the valence band to another Fe level. Therefore, doped Fe-TiO_2 photocatalysts have narrower band gap than pure TiO_2 and could increase the absorption in the visible-light region. Subsequently, the departed electrons and holes migrate to the surface of catalyst and react with

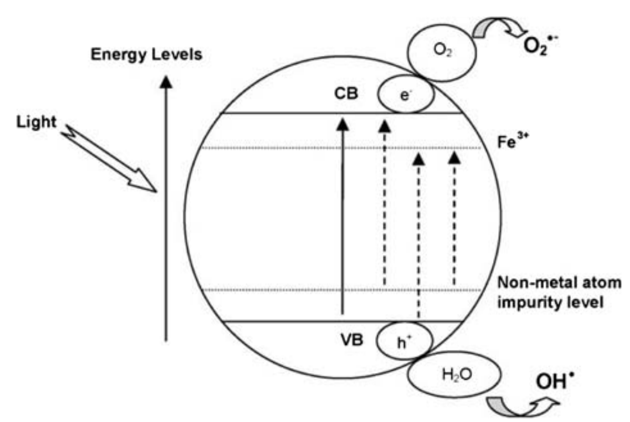

Fig. 6. Schematic diagram of doped-TiO_2 and initial redox process after activation by light [6,13].

adsorbed O_2 and H_2O, respectively, forming $O_2^{\bullet}$ and $^{\bullet}OH$, the main species responsible for the degradation of pollutants [6,13], such as phenol in our case.

Dopant concentration plays also an important role in the activity of final product. It is known that the electron–hole recombination rate (k_{recomb}) in Fe-doped TiO_2 is described by equation $k_{\text{recomb}}/\exp\,(2R/a_0)$, where a_0 is the radius of the hydrogenic wave function of the trapped carriers and R is the average distance between the separated electrons and holes [6,16,17]. Consequently, k_{recomb} exponentially increases with the Fe^{3+} concentration in the TiO_2, because R decreases with the increasing amount of Fe^{3+} dopant. Concentration below the optimal value, there are fewer trapping sites available and Fe^{3+} serves as shallow trapping sites for charge carrier (e^- or h^+), thereby separating the arrival time of e^- and h^+ at the surface and increasing the efficiency [8]. On the other hand, at high concentration, these trapped e^- or h^+ might recombine together before migrating to the surface, resulting in lower photocatalytic activity of TiO_2. Thus, the efficiency is strongly associated with Fe^{3+} concentration [18].

In general, the activity of Fe-doped TiO_2 photocatalyst under solar irradiations was found to be higher than that under pure visible irradiation (Fig. 5). This might be attributed to the fact that solar light contains 4% of UV. This portion of UV light is responsible for the activation of titania particles that are not in contact with iron and hence more active sites are available for radicals production.

3.3. Effect of catalyst concentration

The effect of catalyst weight on the percentage removal of phenol was investigated at 50–250 ppm catalyst concentration. Pseudo-first-order kinetics is plotted in Fig. 7 and calculated rate constants are

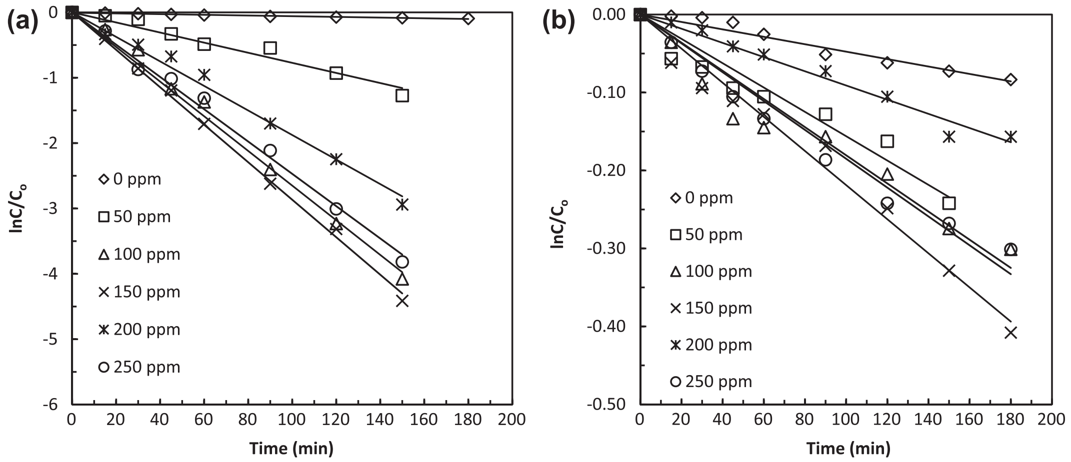

Fig. 7. Effect of catalyst concentration on phenol degradation using 0.05% Fe/Ti doping ratio under (a) sunlight and (b) pure visible irradiation.

Table 1
Rate constants of pseudo-first-order reaction of phenol degradation under visible and sunlight irradiations for 0.05% Fe/Ti doping ratio at different catalyst doses

Catalyst dose	Visible irradiation			Solar irradiation		
(ppm)	k_{app} (min^{-1})	φ_{180}[a]	R^2	k_{app} (min^{-1})	Φ_{180}	R^2
0	0.00048	8	0.957	0.00057	9	0.969
50	0.00156	17	0.918	0.00772	87	0.960
100	0.00181	26	0.924	0.0265	99.78	0.991
150	0.00219	33.5	0.978	0.02866	100	0.998
200	0.00091	14.5	0.978	0.01876	100	0.989
250	0.00185	26	0.964	0.00247	100	0.993

[a] φ is the efficiency of % phenol removals at optimum reaction time.

presented in Table 1. The results clearly showed that the increase of catalyst weight from 50 to 150 ppm increased the phenol removal percentage sharply from 17 to 33.5% and from 87 to 100% at 180 min under pure visible and solar irradiations, respectively. The low phenol degradation percentage at lower TiO_2 loading can be attributed to the fact that more light is transmitted through the reactor and the transmitted light is not utilized in the photocatalytic reaction [19]. At 150 ppm of TiO_2, enhancement in percentage degradation of phenol is due to (i) the increase in the amount of catalyst weight which increases the number of phenol adsorbed and (ii) the increase in the density of particles in the area of illumination leading to more active radicals. Increasing catalyst concentration to be more than 150 ppm led to slight decrease in rate of phenol degradation which might be due to deactivation of activated molecules by collision with ground-state molecules as well as shielding that may take place by TiO_2. Moreover, increment of catalyst loading can increase the number of active sites but decrease penetration of solar light due to shielding effect [20,21].

3.4. Effect of hydrogen peroxide

One possible way to increase the reaction rate is to increase the concentration of $^{\cdot}OH$ because these species are widely considered to be promoters of photocatalytic degradation. The effect of H_2O_2 addition on the photocatalytic oxidation of phenol was investigated in Fig. 8 using different initial concentrations of H_2O_2 and 0.05% Fe/Ti doping ratio under visible and solar irradiations. The calculated rate constants are

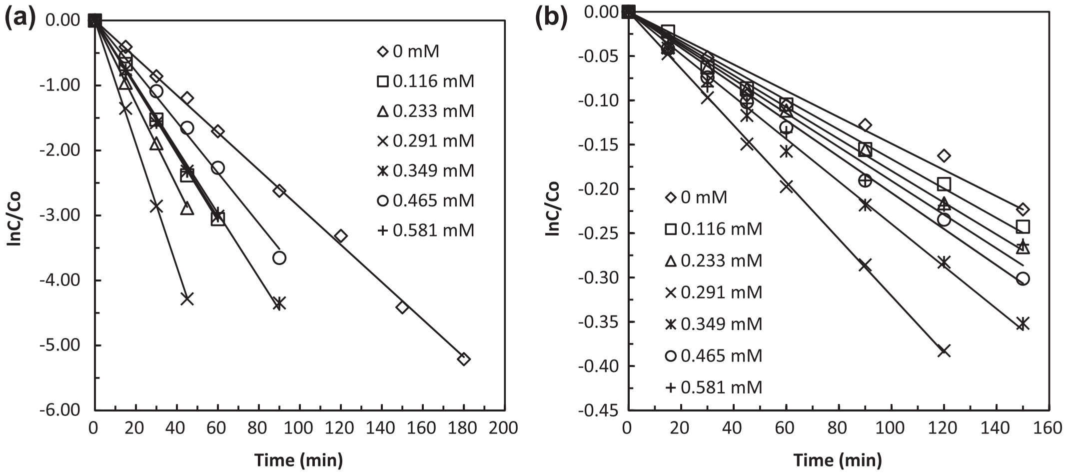

Fig. 8. Effect of H_2O_2 dose on pseudo-first order rate constant of phenol degradation (a) sunlight and (b) pure visible light irradiations using 0.05% Fe/Ti doping ratio.

Table 2
Effect of H_2O_2 dose on pseudo-first-order reaction rate constant of phenol degradation under visible and solar light irradiations for 0.05% Fe/Ti doping ratio

H_2O_2 (mM)	Visible irradiation			Solar irradiation		
	K ($\times 10^{-3}$ min^{-1})	φ_{150}[a]	R^2	k_0 ($\times 10^{-2}$ min^{-1})	Φ_{90}	R^2
0	1.490	20.000	0.962	2.850	92.727	0.997
0.116	1.660	21.547	0.991	5.130	100.000	0.997
0.233	1.800	23.333	0.994	6.380	100.000	1.000
0.291	3.200	34.426	0.999	9.480	100.000	0.999
0.349	2.400	29.648	0.996	4.950	98.705	0.998
0.465	2.040	26.020	0.991	3.910	97.409	0.995
0.581	1.910	23.121	0.995	5.060	100.000	0.998

[a] φ is the efficiency of % phenol removals at optimum reaction time.

presented in Table 2. The results revealed that hydrogen peroxide has a beneficial effect on phenol degradation at low H_2O_2 concentrations (up to 0.291 mM) while high concentration retards photocatalytic degradation of phenol. This is because hydrogen peroxide is considered to have two functions in the process of photocatalytic degradation since it accepts the photogenerated electrons from the conduction band so it promotes charge separation meanwhile; it forms $^{\cdot}OH$ by self-splitting under UV irradiation [22,23]. However, more hydrogen peroxide retarded the progress of reaction. This may be due to autodecomposition of H_2O_2 to oxygen and water and the recombination of $^{\cdot}OH$ [24].

$$2H_2O_2 \rightarrow 2H_2O + O_2$$

$$HO^{\cdot} + H_2O_2 \rightarrow H_2O + HO_2^{\cdot}$$

Since the $^{\cdot}OH$ reacts with H_2O_2, the H_2O_2 itself contributes to the $^{\cdot}OH$ scavenging [25]. Therefore, H_2O_2 should be added at the optimal concentration to achieve the best degradation as the number of hydroxyl radicals generated in the photoreaction is directly proportional to the hydrogen peroxide concentration.

4. Conclusions

Fe-doped TiO_2 photocatalysts of different Fe/Ti molar ratios could be prepared using wet impregnation method. Prepared Fe-doped TiO_2 photocatalysts contain only anatase titania phase while no phase relevant to iron was detected. Photodegradation of phenol using Fe-doped TiO_2 photocatalysts was found to rely on doping ratio. 0.005% Fe/Ti molar ratio exhibited the highest activity due to successful charge separation. In general, prepared photocatalyst was more active under sunlight than pure visible light due to the activation of more particles that are not in contact with iron by UV portion in solar light. Hydrogen peroxide was successfully used to enhance phenol photodegradation by Fe-doped TiO_2.

References

[1] F.B. Li, X.Z. Li, M.F. Hou, Photocatalytic degradation of 2-mercaptobenzothiazole in aqueous La^{3+}—TiO_2 suspension for odor control, Appl. Catal. B. 48 (2002) 185–194.

[2] G. Yu, J.C. Yu, W.K. Ho, M.K. Leung, B. Cheng, G.K. Zhang, X.J. Zhao, Effects of alcohol content and calcination temperature on the textural properties of bimodally mesoporous titania, Appl. Catal. A. 255 (2003) 309–320.

[3] T. Hong, Z.P. Wang, W.M. Cai, F. Lu, J. Zhang, Y.Z. Yang, N. Ma, Y.J. Liu, Visible-light-activated nanoparticle photocatalyst of iodine-doped titanium dioxide, Chem. Mater. 17 (2005) 1548–1552.

[4] J.C. Yu, J.G. Yu, W.K. Ho, Z.T. Jiang, L.Z. Zhang, Effects of Fe—doping on the photocatalytic activity and microstructures of nanocrystalline TiO_2 powders, Chem. Mater. 14 (2002) 3808–3816.

[5] J.G. Yu, H.G. Ao, C.H. Yu, S.C. Lee, J.C. Yu, W.K. Ho, Preparation, characterization and photocatalytic activity of *in situ* Fe-doped TiO_2 thin films, Thin Solid Films 496 (2006) 273–280.

[6] M. Zhou, J. Yu, B. Cheng, H. Yu, Preparation and photocatalytic activity of Fe-doped mesoporous titanium dioxide nanocrystalline photocatalysts, Mater. Chem. Phys. 93 (2005) 159–163.

[7] J. Wang, W. Suna, Z. Zhang, Z. Jianga, X. Wang, R. Xua, R. Li, X. Zhang, Preparation of Fe-doped mixed crystal TiO_2 catalyst and investigation of its sonocatalytic activity during degradation of azo fuchsine under ultrasonic irradiation, J. Colloid Interface Sci. 320 (2008) 202–209.

[8] M.S. Nahar, K. Hasegawa, S. Kagaya, Photocatalytic degradation of phenol by visible light-responsive iron-doped TiO_2 and spontaneous sedimentation of the TiO_2 particles, Chemosphere 65 (2006) 1976–1982.

[9] Eddy & Metcalf Inc., Wastewater Engineering Treatment and Reuse, fourth ed., McGraw-Hill, New York, NY, 2003.

[10] G. Zhao, H. Kozuka, H. Lin, T. Yoko, Sol–gel preparation of $TixVxO_2$ solid solution film electrodes with conspicuous photo response in the visible region, Thin Solid Films 339 (1999) 123–128.

[11] K. Iketani, K. Hirota, O. Yamaguchi, R.D. Sun, M. Toki, Sol–gel-derived $VxTixO_2$ films and their photocatalytic activities under visible light irradiation, Mater. Sci. Eng. B 108 (2004) 187–193.

[12] N. Uekawa, Y. Kurashima, K. Kakegawa, Y. Sasaki, Preparation and nonstoichiometric property of wide compositional Fe(III)-doped TiO_2 (anatase), J. Mater. Res. 15 (2000) 967–973.

[13] W. Choi, A. Termin, M.R. Hoffmann, The role of metal ion dopants in quantum-sized TiO_2: Correlation between photoreactivity and charge carrier recombination dynamics, J. Phys. Chem. 98 (1994) 13669–13679.

[14] H. Ogawa, A. Abe, M. Nishikawa, S. Hayakawa, Preaparation of Tin oxide films from ultrafine particles, Electro. chem. Soc. 128 (1981) 685–689.

[15] M.C. Wang, H.J. Lin, T.S. Yang, Characteristics and optical properties of iron ion (Fe^{3+})-doped titanium oxide thin films prepared by a sol–gel spin coating, J. Alloy. Compd. 473 (2009) 394–400.

[16] M. Grätzel, Heterogeneous Photochemical Electron Transfer Reaction, CRC Press, Boca Raton, FL, 1987.

[17] S.M. Oh, S.S. Kim, J.E. Lee, T. Ishigaki, D.W. Park, Effect of additives on photocatalytic activity of titanium dioxide powders synthesized by thermal plasma, Thin Solid Films 435 (2003) 252–258.

[18] T.A. Gad Allah, S. Kato, S. Satokawa, T. Kojima, Effect of carbon coating of TiO_2/Fe_3O_4 particles on their photocatalytic activity, Int. J. Chem. React. Eng. 6 (2008) A15.

[19] M. Saquib, M. Muneer, Photocatalytic degradation of the textile dye, alizarin red S, in aqueous suspension of titanium dioxide, Adv. Color Sci. Technol. 5 (2002) 71–78.

[20] R. Terazian, N. Serpone, Heterogeneous photocatalysed oxidation of creosote components: Mineralization of xylenols by illuminated TiO_2 in oxygenated aqueous media, J. Photochem. Photobiol. A Chem. 89 (1995) 163–175.

[21] M. Goncalve, A. Oliveira-Compos, E. Pinto, P. Plasencia, M. Queiroz, Photo–chemical treatment of solutions of azo dyes containing TiO_2, Chemosphere 39 (1999) 781–786.

[22] N. Mahmoodi, M. Arami, L. Yousefi, T. Salman, Decolorization and aromatic ring degradation kinetics of direct red 80 by UV oxidation in the presence of hydrogen peroxide utilizing TiO_2 as photocatalyst, Chem. Eng. J. 112 (2005) 191–196.

[23] N. Mahmoodi, M. Arami, N. Limaee, N. Tabrizi, Kinetics of heterogeneous photocatalytic degradation of reactive dyes in animmobilized TiO_2 photocatalytic reactor, J. Colloid Interface Sci. 295 (2006) 159–164.

[24] M.I. Badawy, M.Y. Ghaly, T.A. Gad-Allah, Advanced oxidation processes for the removal of organophosphorus pesticides from wastewater, Desalination 194 (2006) 166–175.

[25] G.V. Buxton, C.L. Greenstock, W.P. Helman, A.B. Ross, Critical review of rate constants for reaction of hydrated eletrons, hydrogen atoms and hydroxyl radicals ($^{\bullet}OH/O^{\bullet}$) in aqueous solution, J. Phys. Chem. Ref. Dat. 17 (1988) 513–886.